

Deep-water gravity waves: theoretical estimating of wave parameters

I. M. Mindlin

State Technical University of Nizhny Novgorod, Russia

E-mail address: ilia.mindlin@gmail.com

This paper addresses deep-water gravity waves of finite amplitude generated by an initial disturbance to the water. It is assumed that the horizontal dimensions of the initially disturbed body of the water are much larger than the magnitude of the free surface displacement in the origin of the waves.

Initially the free surface has not yet been displaced from its equilibrium position, but the velocity field has already become different from zero. This means that the water at rest initially is set in motion suddenly by an impulse.

Duration of formation of the wave origin and the maximum water elevation in the origin are estimated using the arrival times of the waves and the maximum wave-heights at certain locations obtained from gauge records at the locations, and the distances between the centre of the origin and each of the locations.

For points situated at a long distance from the wave origin, forecast is made for the travel time and wave height at the points. The forecast is based on the data recorded by the gauges at the locations.

1. Problem outline.

In the present study the deep-water waves are considered which start to propagate away from an initially disturbed body of water. Then the water is acted on by no external force other than gravity. It is assumed that the free surface of the water is infinite in extent and the pressure along the surface is constant. It is also assumed that the horizontal dimensions of the initially disturbed body of water are much larger than the maximum water elevation in the wave origin.

Below the case of plane waves is discussed. A sketch of the flow is shown in figure 1, where (x, y) -plane is the plane of flow, the x -axis is oriented upward and the y -axis in horizontal direction. Let the curve Γ be the trace of the free surface S in the (x, y) plane, $x = f < 0$, $y = 0$ be the coordinates of the pole O_1 of the polar coordinate system in the (x, y) plane, θ be the polar angle measured from the positive x -axis in the counterclockwise direction, t be the time. The external pressure, P_* , on the free surface is constant. The liquid fills the space below the free surface. The equilibrium position of the free surface is in horizontal plane $x = 0$

Equations to the problem are presented in [1] and [2].

We begin by summarizing very briefly the pertinent theoretical results that we need. The results for plane waves are proved, for instance, in [2].

2. Preliminaries

2.1. The equations of the free surface

The equations of the free surface are obtained in parametric form as follows

$$x = cW_0(\theta, t), \quad y = (x - f) \tan \theta, \quad -\pi/2 < \theta < \pi/2 \quad (2.1.1)$$

$$W_0(\theta, t) = \sum_{n=1}^{+\infty} (-1)^{n-1} \frac{1}{2n} [a_n I_{2n+1}(\tau, \theta) + b_n J_{2n+1}(\tau, \theta)] + \quad (2.1.2)$$

$$\frac{1}{\sqrt{2|f|}} \sum_{n=1}^{+\infty} (-1)^n [\rho_n P_{2n}(\tau, \theta) + e_n Q_{2n}(\tau, \theta)], \quad t = \tau \sqrt{2|f|}$$

$$I_{2n+1}(\tau, \theta) = \int_0^{+\infty} x^{2n+1} e^{-x^2/2} \cos\left(\frac{1}{2}x^2 \tan \theta\right) \cos(\tau x) dx; \quad (2.1.3)$$

$$J_{2n+1}(\tau, \theta) = \int_0^{+\infty} x^{2n+1} e^{-x^2/2} \sin\left(\frac{1}{2}x^2 \tan \theta\right) \cos(\tau x) dx; \quad (2.1.4)$$

$$P_{2n}(\tau, \theta) = \int_0^{+\infty} x^{2n} e^{-x^2/2} \cos\left(\frac{1}{2}x^2 \tan \theta\right) \sin(\tau x) dx; \quad (2.1.5)$$

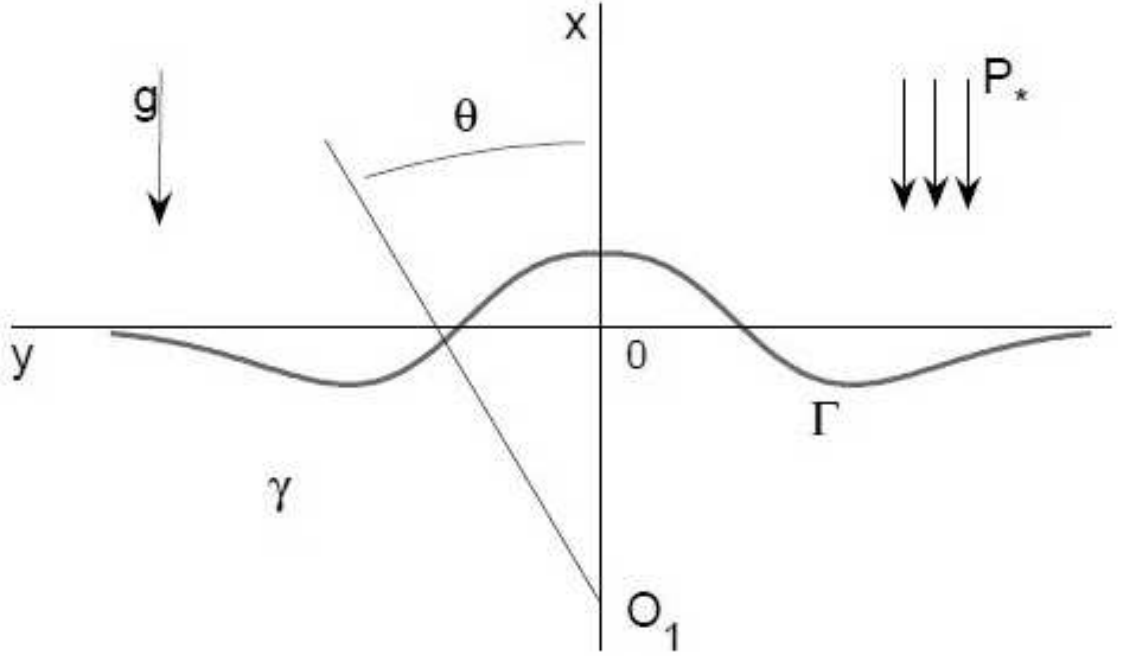


Figure 1: Coordinate systems and sketch of the free surface of a liquid.

$$Q_{2n}(\tau, \theta) = \int_0^{+\infty} x^{2n} e^{-x^2/2} \sin\left(\frac{1}{2}x^2 \tan \theta\right) \sin(\tau x) dx. \quad (2.1.6)$$

The constants a_n, b_n determine the initial displacement to the free surface, the initial velocity field is determined by the constants ρ_n, e_n . The constants are independent of f .

Formally, equations (2.1.1) for each specified function W_0 describe a family of curves depending on f, t being considered as constant. The value of f determines the horizontal scale of the problem.

Let c be the maximum of the free surface displacement in the wave origin, so $\varepsilon = c/f$ is the ratio of the maximum displacement to the characteristic horizontal dimension of the origin. The problem was solved approximately up to small terms of order of $\varepsilon = c/f$.

2.2. Zeros of the wave group and terminology

Zeros of the wave group (2.1.1) are defined by the equation $W_0 = 0$ and (at fixed value of τ) are situated in the numbered rays $\theta = \theta_k(\tau)$ (k is the number of a zero). For brevity we will use the term 'zero $\theta(\tau)$ ' to denote a zero of a wave. Zeros $\theta_k(\tau)$ of the wave group are independent of f .

The term 'wave' means a wave-group's section which is singled out by three zeros and consists of a crest and the trough following or preceding the crest. The level difference between the crest and the trough is referred to as the wave height (or height of the wave), and the distances between two successive zeros is "half-wave-length".

At any particular moment of time, each specific wave packet contains only one wave of maximum height (WMH) on semiaxis $y > 0$ (the situation with two waves of equal maximum height can be ignored), so the zeros of WMH constitute a 'natural frame of reference' for other zeros: let the zero θ_1 be the front of the WMH, the zero θ_{-1} be the rear of the WMH, and the zero θ_0 be between the crest and the trough of the WMH; the distance between zeros θ_{-1} and θ_1 is the length l of the WMH: $l = |f \tan \theta_1 - f \tan \theta_{-1}|$. Calculations show that

$$|\tan \theta_1 - \tan \theta_{-1}| \approx 5 \quad \text{for } 30 < \tau < 640. \quad (2.2.1)$$

All equations are written in non-dimensional variables. Since the problem has no characteristic linear size, the dimensional unit of length, L_* , is a free parameter. But in the section 5, the value

of L_* , as well as the value of $|f|L_*$, will be obtained from instrumental data. The dimensional unit of time, T_* , is defined by the relation $T_*^2 g = L_*$, where g is the acceleration of free fall. The non-dimensional acceleration of free fall is equal to unity. All parameters, variables and equations are made non-dimensional by the quantities L_* , T_* , P_* and the density of water $\gamma = 1000 \text{ kg/m}^3$.

2.3. Specific wave packets

Specific wave packets are defined by equations

$$x = I_{2n+1}, \quad y = (x - f) \tan \theta \quad (2.3.1)$$

$$I_{2n+1}(\tau, \theta) = \int_0^{+\infty} x^{2n+1} e^{-x^2/2} \cos\left(\frac{1}{2}x^2 \tan \theta\right) \cos(\tau x) dx;$$

The subscript $2n + 1$ is referred to as the packet number.

In [2] the sequence of instantaneous forms of specific packets number 5, 23, and the mixture of the two packets at $\tau = 25, 50, 100, 200,$ and 300 is shown. We can see from the sequence of forms that the greater the packet number, the shorter the wavelength of its WMH, the slower the packet travels, the slower the packet disperses. It is clear from the sequence of instantaneous forms that the packet is growing in length. Three parts of the packet are observed on the surface, namely, the leading part of small amplitude which is followed by a middle part of larger amplitude; the "tail" of the packet is relatively short

Equations of other three sets of wave packets are obtained from (2.1.1), (2.1.2), (2.1.4) - (2.1.6).

By equations (2.1.1) - (2.1.6), any wave group on the free surface is a mixture of finite or infinite (it depends on initial conditions) set of the specific wave packets of different numbers, and evolution of each packet in the mixture is not influenced by evolution of the others.

3. Gauge records and data extracted from the records

In next sections a procedure is demonstrated for estimating some parameters of waves using arrival times of the waves of maximum height and their heights obtained from gauge records at some locations. To be assured that the horizontal dimensions of the wave origin are much larger than the magnitude of the free surface displacement in the origin, we use tsunami records at DART buoys deployed in the Pacific Ocean at a depth of 5000 metres. Records of the buoys and their locations can be found on the USA National Data Buoy Center public website (<http://www.ndbc.noaa.gov/dart.shtml>).

Figure 2 shows the Peruvian 08/2007 tsunami records de-tided using low-pass Butterworth filter with 150 min cut-off; the residuals are non-tidal components, i.e., the mixture of seismic signal (of shorter period) and the tsunami waves.

Data extracted from the records at the DARTS are summarized in Tables 1 - 3, where the travel time of the MHW, t_* min, the maximum wave-height, H_* cm, and the distance between the gauge sensors and the centre (epicentre of the earthquake) of the wave origin, y_* km, are shown for each of the DARTs.

TABLE 1. The Peruvian tsunami: WMH as recorded at the DART buoys.

i	Buoy	t_* min.	H_* cm	y_* km	y_*/t_*^2
1	32401	49	7.0	713	0.296960
2	32411	198	1.7	2561	0.065325
3	51406	444	3.9	5320	0.026986
4	46412	624	2.0	6921	0.017775

Figure 3 and Table 2 show the de-tided Dart records and data for tsunami triggered by the earthquake near Kuril Islands in January 2007.

TABLE 2. The 2007 Kuril tsunami: WMH as recorded at the DART buoys.

Buoy	t_* min.	H_* cm	y_* km	y_*/t_*^2
21413	120	4.0	1762	0.122361
21414	120	5.7	1804	0.125278
46413	154	5.7	2253	0.094999
46408	200	4.5	2660	0.066500
46419	438	1.6	5470	0.028513

Tsunami was generated by the the earthquake occurred near Kuril Islands in November 2006.

The data obtained from the DART records of the tsunami are shown in Table 3.

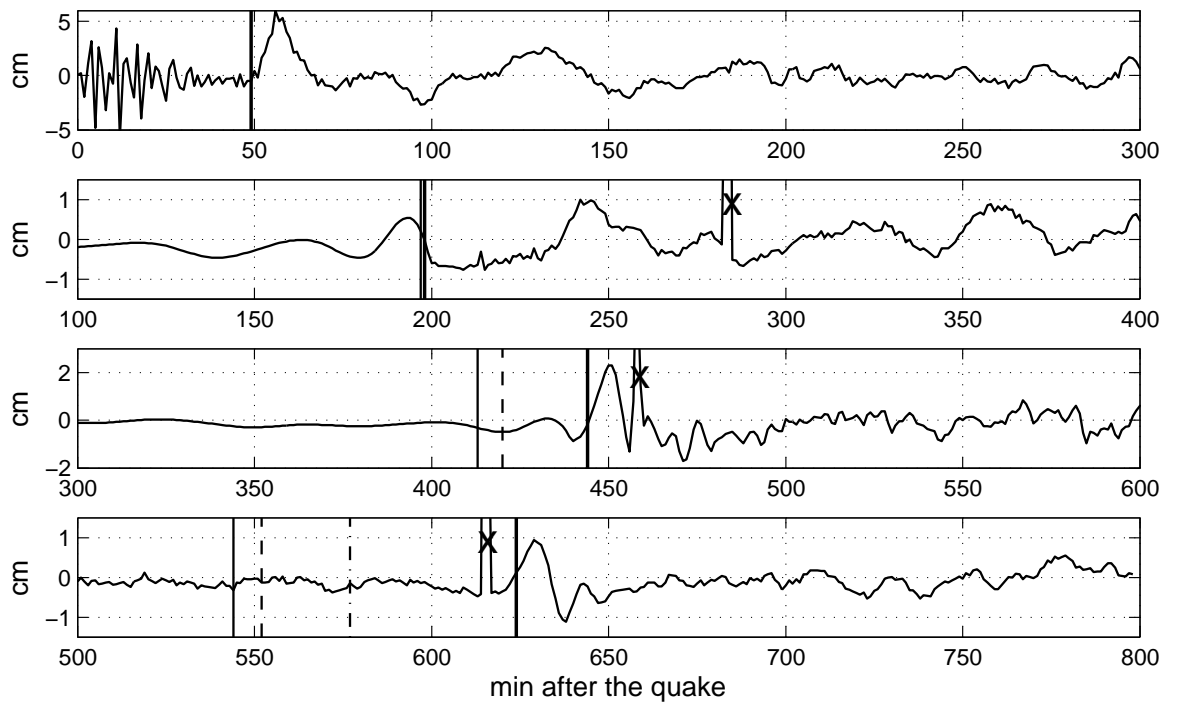


Figure 2: De-tided records of the Peruvian 08/2007 tsunami at DART buoys (top to bottom) 32401, 32411, 51406, 46412. Vertical lines mark the arrival of the front of the WMH (thick solid line), its estimate with the first buoy record for the next three buoys (thin solid), its estimate with the first and second buoy records for the next two buoys (dashed), its estimate with the three buoys for the last one (dashdot). Crosses mark trigger pulses (signals send by an operator).

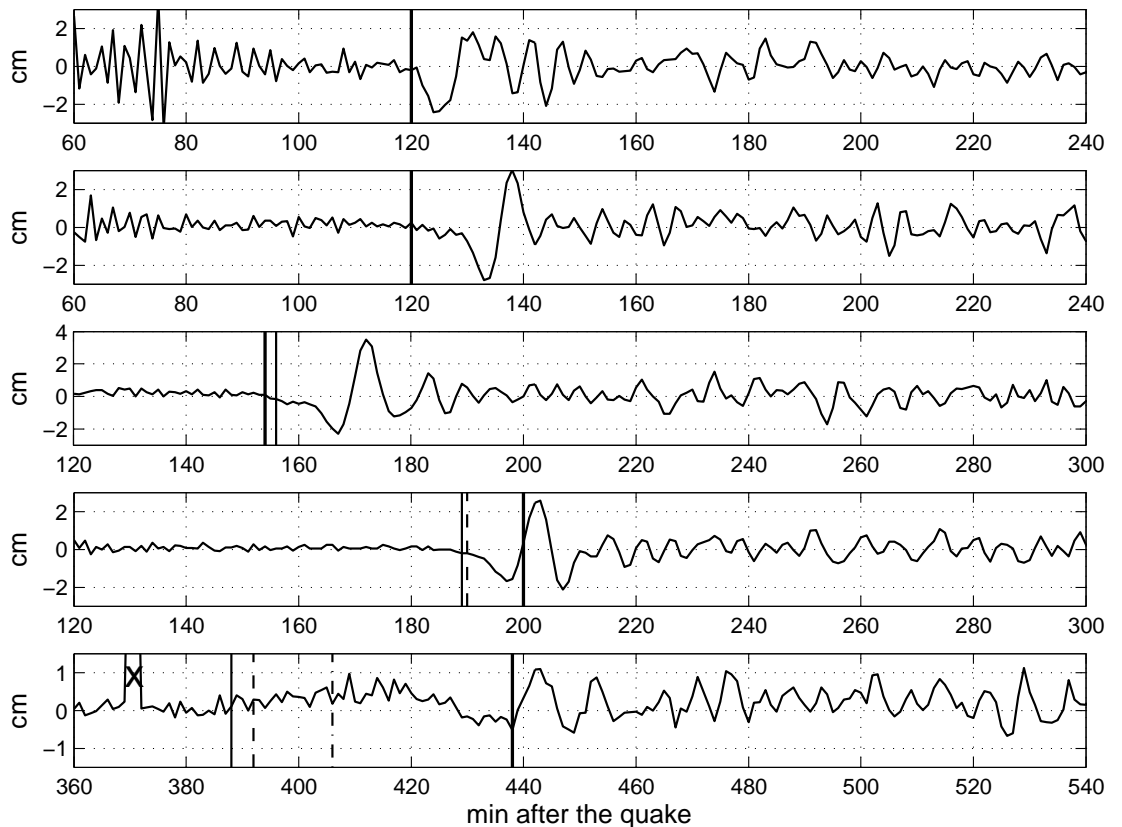


Figure 3: De-tided records of the Kuril 01/2007 tsunami at DART buoys (top to bottom) 21413, 21414, 46413, 46408, 46419. Vertical lines mark the arrival of the front of the WMH (thick solid line), its estimate with the first and second buoy records for the next three buoys (thin solid), its estimate with the first three buoy records for the next two buoys (dashed), its estimate with the four buoys for the last one (dashdot). Cross marks a trigger pulse (signals send by an operator).

TABLE 3. The 2006 Kuril tsunami: WMH as recorded at the DART buoys.

	Buoy	t_* min.	H_* cm	y_* km	y_*/t_*^2
Data 3.	46413	155	8.5	2331	0.097024
	46408	238	7.5	2735	0.048284
	46402	270	10.0	3127	0.042894
	46403	365	7.5	3581	0.026879

4. Estimation of some parameters

4.1. Model for the waves recorded

Assume the surface waves are described by equations

$$x = c \frac{1}{\sqrt{2|f|}} P_2, \quad y = (x - f) \tan \theta \quad (4.1.1)$$

$$P_2(\tau, \theta) = \int_0^{+\infty} x^2 e^{-x^2/2} \cos\left(\frac{1}{2}x^2 \tan \theta\right) \sin(\tau x) dx.$$

By the moment $t = 0$ the free surface has not yet been displaced from its mean level (the horizontal plane $x = 0$), but the velocity field has already become different from zero. This means that the motion of a body of water is triggered by a sudden change in the velocity field. The wave packet (4.1.1) travels faster than any other specific packet.

4.2. Properties of the specific wave packet (4.1.1)

Horizontal coordinate of the zero $\theta_k(\tau)$ is given by $y_k = -f \cdot \tan \theta_k(\tau)$ and the function $P_2(\tau; \theta)$ is independent of f . This leads to the following

Assertion: At any given value of τ

i) for any wave of the packet the quantity $\Delta(\tau) = h(\tau)\sqrt{2|f|}$ ($h(\tau)$ is the height of the wave) is independent of f ;

ii) the ratio of the distances $y_{k+1}(\tau) - y_k(\tau)$ and $y_k(\tau) - y_{k-1}(\tau)$ between any successive zeros of the wave packet (and, consequently, the ratio of the lengths of two successive waves) is independent of f .

Let L_* be the dimensional unit of length (in metres), then $T_* = \sqrt{L_*/g}$ is the dimensional unit of time (in seconds).

At an instant t_* the dimensional coordinate of any zero $\theta = \theta(\tau)$ is

$$y_*(t_*) = |f|L_* \cdot \tan \theta(\tau) \cdot 10^{-3} \text{ km}, \quad t_* = \tau \sqrt{2|f|} \cdot T_*/60 \text{ min},$$

and, consequently, the ratio

$$\lambda(\tau) = \frac{y_*(t_*)}{t_*^2} \text{ km/min}^2 = 17.64 \frac{\tan \theta(\tau)}{\tau^2} \text{ km/min}^2. \quad (4.2.1)$$

depends on τ only.

Given a fixed value of τ , $\tan \theta(\tau)$ can be calculated from equations (4.1.1) of the wave packet, and corresponding value of $\lambda(\tau)$ can be obtained from (4.2.1).

Let $\theta_1(\tau)$ denote one of the three zeros $\theta(\tau)$ of the WMH, which corresponds to maximum of the three $|\tan \theta(\tau)|$. By the zero $\theta_1(\tau)$ we define the front of WMH (see subsection 2.2).

Table 4 shows computed characteristics of the WMH: $\tan \theta_1$, $\lambda(\tau)$, and $\Delta(\tau) = H(\tau)\sqrt{2|f|}$ ($cH(\tau)$ is the maximum wave height) obtained from (4.1.1) and (4.2.1) (at $c = 1$ $f = -10$).

TABLE 4. Computed characteristics of the wave of maximum height.

τ	25	30	35	40	45	50
$\tan \theta_1$	19.032	19.818	23.687	27.587	31.508	32.531
λ	0.5371	0.3884	0.3411	0.3041	0.2744	0.2295
$\Delta(\tau)$	0.6326	0.5927	0.5653	0.5380	0.5126	0.4911
$\lambda \cdot \tau$	13.429	11.653	11.938	12.166	12.351	11.477
u		0.1572	0.7738	0.7800	0.7842	0.2046
τ	55	60	65	70	75	80
$\tan \theta_1$	36.396	40.268	44.159	48.057	49.114	52.974
λ	0.2122	0.1973	0.1844	0.1730	0.1540	0.1460
$\Delta(\tau)$	0.4738	0.4577	0.4420	0.4267	0.4155	0.4035
$\lambda \cdot \tau$	11.673	11.839	11.984	12.110	11.552	11.681
u	0.7730	0.7744	0.7782	0.7796	0.2114	0.7720

τ	90	100	110	120	130	140
$\tan \theta_1$	58.000	65.695	70.734	78.421	83.470	88.559
λ	0.1263	0.1159	0.1031	0.0960	0.0871	0.0797
$\Delta(\tau)$	0.3840	0.3661	0.3507	0.3371	0.3255	0.3152
$\lambda \cdot \tau$	11.368	11.589	11.343	11.528	11.326	11.158
u	0.5026	0.7695	0.5039	0.7687	0.5049	0.7606

τ	150	160	170	180	200	220
$\tan \theta_1$	96.203	101.294	108.935	116.607	126.767	142.072
λ	0.0754	0.0698	0.0665	0.0635	0.0559	0.0518
$\Delta(\tau)$	0.3050	0.2960	0.2884	0.2804	0.2676	0.2554
$\lambda \cdot \tau$	11.313	11.168	11.304	11.427	11.181	11.391
u	0.7644	0.5091	0.7641	0.7672	0.5081	0.7652

τ	240	260	280	300	310	320
$\tan \theta_1$	154.802	167.532	180.265	192.996	198.071	205.727
λ	0.0474	0.0437	0.0406	0.0378	0.0364	0.0354
$\Delta(\tau)$	0.2446	0.2367	0.2281	0.2204	0.2175	0.2141
$\lambda \cdot \tau$	11.378	11.357	11.357	11.348	11.271	11.341
u	0.6365	0.6366	0.6366	0.6365	0.5075	0.7656

τ	330	340	360	370	380	390
$\tan \theta_1$	210.802	218.458	231.189	236.267	243.920	249.002
λ	0.0341	0.0333	0.0315	0.0304	0.0298	0.0289
$\Delta(\tau)$	0.2108	0.2077	0.2019	0.1991	0.1965	0.1950
$\lambda \cdot \tau$	11.268	11.334	11.328	11.264	11.323	11.262
u	0.5075	0.7656	0.6365	0.5078	0.7653	0.5082

τ	400	410	420	440	460	470
$\tan \theta_1$	254.094	261.734	269.387	279.559	292.291	299.931
λ	0.0280	0.0275	0.0269	0.0255	0.0244	0.0239
$\Delta(\tau)$	0.1926	0.1902	0.1879	0.1836	0.1796	0.1776
$\lambda \cdot \tau$	11.205	11.261	11.314	11.208	11.209	11.257
u	0.5092	0.7640	0.7653	0.5086	0.6366	0.7640

5

τ	480	490	500	520	540	550
$\tan \theta_1$	305.023	312.663	317.762	330.494	343.227	350.867
λ	0.0233	0.0230	0.0224	0.0216	0.0208	0.0205
$\Delta(\tau)$	0.1758	0.1744	0.1729	0.1706	0.1674	0.1659
$\lambda \cdot \tau$	11.209	11.256	11.211	11.211	11.212	11.253
u	0.5092	0.7640	0.5099	0.6366	0.6366	0.7640

τ	560	580	600	620	630	640
$\tan \theta_1$	355.959	368.691	381.424	394.155	401.796	406.888
λ	0.0200	0.0193	0.0187	0.0181	0.0178	0.0175
$\Delta(\tau)$	0.1644	0.1616	0.1588	0.1563	0.1550	0.1538
$\lambda \cdot \tau$	11.213	11.213	11.214	11.214	11.250	11.215
u	0.5092	0.6366	0.6366	0.6365	0.7641	0.5092

In Table 4, values of the ratios $u = \Delta \tan \theta_1 / \Delta \tau$ are given for each two neighbouring columns (for instance, for the columns $\tau = 25$ and $\tau = 30$ we find $u = (19.818 - 19.032)/(30 - 25) = 0.1572$).

During a time interval t_* min, the front of the WMH travels a distance $y_*(t_*)$ km at the average speed

$$V_* = \frac{y_*(t_*)}{t_*} = \lambda(\tau) \cdot \tau \sqrt{2|f|} \cdot \frac{T_*}{60} \text{ km/min.} \quad (4.2.2)$$

The value of the front's average speed during time interval $\Delta \tau = \tau_{n+1} - \tau_n$ equals

$$v_* = u \sqrt{|f|L_*g/2}, \quad u = [\tan \theta_1(\tau_{n+1}) - \tan \theta_1(\tau_n)] / \Delta \tau, \quad (4.2.3)$$

where τ_n and u are given in Table 4.

The values of $\lambda \tau$ and u seems to suggest that the average speed of the front is nearly constant: in the interval $75 \leq \tau \leq 640$, $\lambda \tau$ ranges from 11.158 to 11.680.

5. Estimation of parameters using wave measurements

5.1. Estimators for the wave model parameters

For the front of the wave of maximum height (as for any zero) the following formulas hold

$$y_*(t_*) = -f \tan \theta_1(\tau) \cdot L_* > 0, \quad t_* = \tau \sqrt{2|f|L_*/g}.$$

If at each locality i data for the waves (4.1.1) were obtained from the records exactly, the functions

$$S(a) = \sum_{i=1}^4 (y_{*i}(t_{*i}) - a \cdot \tan \theta_1(\tau_i))^2 \quad \text{and} \quad F(a) = \sum_{i=1}^4 \left(60t_{*i} - \tau_i \sqrt{\frac{2a}{g}} \right)^2$$

would be equal to zero at $a = |f_*|$, where $|f_*| = |f|L_*$.

But using equations (4.1.1) and values of y_{*i} , t_{*i} , H_{*i} (obtained with errors) we estimate the value of a by minimizing $S(a)$ or $F(a)$.

Minimum value of $S(a)$ occurs at

$$a = |f_{*1}| = \frac{\sum_i y_{*i} \tan \theta_{1i}}{\sum_i \tan^2 \theta_{1i}} \text{ km}, \quad (5.1.1)$$

while minimum value of $F(a)$ is reached at

$$a = |f_{*2}| = \left(\frac{\sum_i t_{*i} \tau_i}{\sum_i \tau_i^2} \cdot 60 \right)^2 4.9 \text{ m}. \quad (5.1.2)$$

In the Table 4, the quantity $\Delta(\tau) = H(\tau)\sqrt{2|f|}$ is independent of f ($cH(\tau)$ is the height of the WMH). If the data in Tables 1 - 3 were measured exactly at each locality i , the function

$$D(s) = \sum_i (c\Delta(\tau_i) \frac{1}{\sqrt{2|f|}} L_* - H_{*i})^2 = \sum_i (\Delta(\tau_i)cs - H_{*i})^2, \quad cs = \frac{1}{\sqrt{2a}} L_*^{3/2}$$

would be equal to zero at true value of s .

At actual values of H_{*i} the value of cs is estimated by minimizing $D(s)$, which leads to the estimator

$$L_*^3 = 2a(c\eta)^2, \quad c\eta = \frac{B}{A}, \quad A = \sum_i \Delta^2(\tau_i), \quad B = \sum_i \Delta_i H_{*i}, \quad (5.1.3)$$

where $c\eta$ is independent of c and f , a is estimated by (5.1.1) or (5.1.2).

5.2. Estimators for the wave parameters

Calculations show that during some time interval, say $0 \leq \tau \leq \tau_1$, a water hill in the form of a rounded solitary elevation symmetric with respect to the vertical x -axis is appearing on the water surface. The height of the hill increases and reaches the maximum at $\tau = \tau_1 = 0.872$. On the interval $0 \leq \tau \leq \tau_1$ there is only one zero $\theta(\tau)$ in the surface (at $y > 0$), and the zero is almost immovable. Only at $\tau > \tau_1$ the heap of water begins to spread out and to turn into a wave group, which runs away from the vertical x -axis. The time interval $0 \leq \tau \leq \tau_1$ is referred to as the interval of formation of the wave origin.

Calculations show that $\max \Delta(\tau) = \Delta(0.842) = 1.036$ (maximum is reached at $\theta = 0$). This means that the maximum of the water elevation in the wave origin is given as

$$h = c\Delta(0.842) L_* / \sqrt{2|f|} \quad \text{or} \quad h = 1.036c\eta, \quad (5.2.1)$$

where $c\eta$ is given by (5.1.3).

Note that the right part of (5.2.1) is independent of c and f .

Duration t of the wave origin formation is estimated by ($g = 9.8 \text{ m/s}^2$, a is measured in metres)

$$t = \tau_1 \sqrt{2|f|L_*/g} \quad \text{or} \quad t = 0.842 \sqrt{2a/g} \text{ s}. \quad (5.2.2)$$

By (2.2.1) length of the WMH is estimated as

$$l_* \approx 5a. \quad (5.2.3)$$

Using formulas (4.2.2) the average speed V of the front of WMH during time interval $0 < \tau < \tau_*$ may be estimated as

$$V_* = \lambda \cdot \tau_* \sqrt{\frac{2a}{g}} \cdot \frac{1}{60} \text{ km/min}; \quad (5.2.4)$$

formula (4.2.3) gives the estimate of the average speed during shorter time interval

$$v_* = u \sqrt{\frac{ag}{2}}. \quad (5.2.5)$$

5.3. Theoretical characteristics of the WMH at locations of the DART buoys.

The Table 4 shows that $\tan \theta_1$ and λ are monotone functions of τ , so for given value of λ the values of τ and $\tan \theta_1$ can be calculated using equations (4.1.1) or estimated using Table 4.

For each DART location, setting $\lambda = y_*/t_*^2$ (see Tables 1 - 3) and using Table 4, we obtain the results, shown in Tables 5 - 7.

TABLE 5. For Data 1: theoretical characteristics of the WMH at locations of the DART buoys.

Dart	λ	τ	$\tan \theta_1(\tau)$	Δ
32401	0.296960	41.206	28.533	0.531882
32411	0.065325	173.917	111.939	0.285267
51406	0.026986	418.567	268.290	0.188230
46412	0.017775	630.833	402.220	0.154900

Values of τ , $\tan \theta_1(\tau)$, $\Delta(\tau)$ in the first line of Table 5 are obtained with the use of $\lambda = 0.296960$ (in the first line of Table 1) and Table 4 as follows. We see from Table 4 that $0, 2744 < \lambda = 0, 296960 < 0, 3041$, $40 < \tau < 45$, $27, 587 < \tan \theta_1(\tau) < 31, 508$, $0, 5126 < \Delta(\tau) < 0, 5380$.

Method of linear interpolation gives $\tau = 41, 202$, $\tan \theta_1(\tau) = 28, 530$, $\Delta(\tau) = 0, 531894$. The rest lines in Table 5 are obtained in the same way.

Tables 6 and 7 are similar to Table 5 and obtained in similar way.

TABLE 6.
For Data 2: theoretical characteristics of the WMH at locations of DART buoys.

Dart	λ	τ	$\tan \theta_1(\tau)$	Δ
21413	0.122361	93.787	60.914	0.374984
21414	0.125278	90.983	58.756	0.378995
46413	0.094999	121.125	78.987	0.335795
46408	0.066500	170.000	108.935	0.288400
46419	0.028513	394.300	251.192	0.193968

Table 7. For Data 3: theoretical characteristics of the plane WMH at locations of the DART buoys.

Dart	λ	τ	$\tan \theta_1(\tau)$	Δ
46413	0.097024	118.558	78.411	0.339047
46408	0.048284	235.888	154.791	0.246741
46402	0.042894	265.038	180.234	0.234534
46403	0.026879	420.300	279.545	0.187836

5.3. Applications of the estimators

Estimates based on Data 1.

Table 1, Table 5, estimators (5.1.1) - (5.1.3) and (5.2.1) - (5.2.5) give

$$a_1 = \frac{713 \cdot 28.533 + 2561 \cdot 111.939 + 5320 \cdot 268.290 + 6921 \cdot 402.220}{28.533^2 + 111.939^2 + 268.290^2 + 402.220^2} = 18,284 \text{ km}$$

$$a_2 = \left(\frac{49 \cdot 41.206 + 198 \cdot 173.917 + 444 \cdot 418.567 + 624 \cdot 630.833}{41.206^2 + 173.917^2 + 418.567^2 + 630.833^2} \right)^2 \cdot 4.9 = 18278 \text{ m}$$

The maximum of the water elevation in the wave origin is $h = 13.5$ cm.

Duration t of the wave origin formation is estimated as

$$t_1 = 0.842\sqrt{2a_1/g} = 51.43 \text{ s}, \quad t_2 = 0.842\sqrt{2a_2/g} = 51.42 \text{ s}.$$

The WMH has the length

$$l_* \approx 91 \text{ km}.$$

It follows from the data of Table 1, that actual values of average speed V_{*i} of the front of WMH (during time interval $0 - t_*$) arrived at the buoys locations i are respectively

$$V_{*1} = \frac{713 \cdot 60}{49} = 873 \text{ km/h}, \quad V_{*2} = 776 \text{ km/h}, \quad V_{*3} = 718 \text{ km/h}, \quad V_{*4} = 665 \text{ km/h}.$$

Using formula (5.2.4) and $a = |f_{*1}| = 18284$ m, $g = 9.8$ m/s² we find

$$V_1 = 0.296960 \cdot 41.206 \cdot \sqrt{\frac{18284}{4.9}} \cdot \frac{1}{60} \text{ km/min} = 12.46 \text{ km/min} = 747 \text{ km/h},$$

$$V_2 = 694 \text{ km/h}, \quad V_3 = 690 \text{ km/h}, \quad V_4 = 685 \text{ km/h}.$$

From Tables 4 and 5, and formula (5.2.5) we find the estimate of the average speed during shorter time interval containing the point t_i .

$$v_i^* = u_i \sqrt{\frac{ag}{2}}$$

For buoy 32401 we have $40 < \tau_1 = 41, 168 < 45$, $u = 0, 7842$, $v_1^* = 845$ km/h. In the same way, for other three buoys we obtain

$$v_2^* = 827 \text{ km/h}, \quad v_3^* = 826 \text{ km/h}, \quad v_4^* = 549 \text{ km/h}.$$

For the packet (4.1.1), the average speed of the wave of maximum height is estimated as $[5v_1^* + 10(v_2^* + v_3^* + v_4^*)]/35 = 749$ km/h.

The value of the parameter $\varepsilon = h/a$ is of order 10^{-5} .

Estimates based on Data 2.

Using Table 2 and Table 6 we find

$$a_1 = 23.256 \text{ km}, \quad a_2 = 23166 \text{ m}.$$

The maximum of the water elevation in the wave origin is $h = 14.4$ cm.

Duration t of the wave origin formation is estimated as

$$t_1 = 58.00 \text{ s}, \quad t_2 = 57.89 \text{ s}.$$

The WMH has the length

$$l_* \approx 116 \text{ km}.$$

It follows from Table 2, that actual values of average speed V_{*i} of the front of WMH (during time interval $0 - t_*$) arrived at the buoys locations i are respectively

$$V_{*1} = 881 \text{ km/h}, \quad V_{*2} = 902 \text{ km/h}, \quad V_{*3} = 878 \text{ km/h}, \quad V_{*4} = 798 \text{ km/h}, \quad V_{*5} = 749 \text{ km/h}.$$

Using formula (5.2.4) and $a = |f_{*1}| = 23256$ m, $g = 9.8$ m/s² we find

$$V_1 = 790 \text{ km/h}, \quad V_2 = 785 \text{ km/h}, \quad V_3 = 793 \text{ km/h}, \quad V_4 = 779 \text{ km/h}, \quad V_5 = 774 \text{ km/h}$$

Estimates based on Data 3.

Using Table 3 and Table 7 we find

$$a_1 = 15.424 \text{ km}, \quad a_2 = 15.785 \text{ m}.$$

The maximum of the water elevation in the wave origin is $h = 33.0$ cm.

Duration t of the wave origin formation is estimated as

$$t_1 = 47.24 \text{ s}, \quad t_2 = 47.79 \text{ s}.$$

The WMH has the length

$$l_* \approx 77 \text{ km}.$$

It follows from Table 3, that actual values of average speed V_{*i} of the front of WMH (during time interval $0 - t_*$) arrived at the buoys locations i are respectively

$$V_{*1} = 902 \text{ km/h}, \quad V_{*2} = 689 \text{ km/h}, \quad V_{*3} = 695 \text{ km/h}, \quad V_{*4} = 589 \text{ km/h}.$$

Using formula (5.2.4) and $a = |f_{*1}| = 15424$ m, $g = 9.8$ m/s² we find

$$V_1 = 645 \text{ km/h}, \quad V_2 = 639 \text{ km/h}, \quad V_3 = 638 \text{ km/h}, \quad V_4 = 634 \text{ km/h}.$$

6. Theoretical forecast for the waves recorded.

For the waves (4.1.1), a line of forecasts of the WMH arrival time and amplitude at some buoys is produced corresponding to the timeline of the DART records.

6.1. The forecast based on Data 1

The forecast based on one DART record.

Based on the measurements on DART buoy 32401, forecast of the travel time of the wave of maximum height that reaches each of the next three buoys and its height is prepared in the following way.

Using the first line of Table 1, the first line of Table 5, and estimators (5.1.1) and (5.1.3) (it is supposed that the WMH has not reached the next three buoys yet) we obtain

$$a = |f_{*1}| = 713/28.533 = 24.989 \text{ km}, \quad c\eta = 13.16 \text{ cm.}$$

For each of the next three buoys $\tan \theta_1 = y_*/a$ is calculated, which is then used to locate the values of τ and Δ between two appropriate consecutive values from Table 4.

Illustration. For the first line of Table 8 we find (for the buoy 32411) $\tan \theta_1 = 713/24.989 = 102.476$. It follows from Table 4 that $101.294 < 102.476 < 108.935$, $160 < \tau < 170$, $0.2884 < \Delta < 0.2960$. Method of linear interpolation gives $\tau = 161.560$, $\Delta(\tau) = 0.294824$.

Then, for each buoy, the travel time of the WMH and its height at the locations of the buoys are estimated by (a is taken in metres)

$$t^* = \frac{\tau}{60} \cdot \sqrt{\frac{2a}{9.8}} \text{ min,} \quad (6.1.1)$$

$$H^* = |x_{max} - x_{min}| = c \frac{\Delta \cdot L_*}{\sqrt{2|f|}} = c\Delta \sqrt{\frac{L_*^3}{2|f_*|}} = \Delta(\tau) \cdot c\eta. \quad (6.1.2)$$

Note that the right hand side of (6.1.2) is independent of c and f .

The forecast results are given in Table 8.

Table 8. For Data 1: the forecast based on one DART record.

Buoy	$\tan \theta_1$	τ	Δ	t^* min	H^* cm
32411	102.486	161.560	0.294824	192	3.9
51406	212.896	332.734	0.209989	396	2.8
46412	277.364	435.685	0.184529	518	2.4

It should be noted that formulas (5.1.1), (5.1.3), (5.2.2), and (5.2.1) are used when the forecast is based on arbitrary number of records.

The forecast based on two DART records. The following results are based on the measurements on DART buoys 32401 and 32411. The forecast is produced for the next two buoys.

The first two lines of Table 1, the first two lines of Table 5, and formulas (5.1.1) and (5.1.3) give

$$a = |f_{*1}| = 23.072 \text{ km}, \quad \eta = 9.17 \text{ cm.}$$

On the same lines as Table 8 we obtained Table 9 (in figure 9, t^* is marked by dashed line).

Table 9. For Data 1: the forecast based on two DART records.

Buoy	$\tan \theta_1$	τ	Δ	t^* min	H^* cm
51406	231.233	360.086	0.201838	411	2.3
46412	301.255	472.600	0.177166	540	2.0

The forecast based on three DART records. The following forecast is based on the measurements on DART buoys 32401, 32411, and 51406.

The first three lines of Table 1, the first three lines of Table 5, and formulas (5.1.1) and (5.1.3) give

$$a = |f_{*1}| = 20.339 \text{ km}, \quad \eta = 9.97 \text{ cm.}$$

Table 10. For Data 1: the forecast based on three DART records.

Buoy	$\tan \Theta$	τ	Δ	t^* min	H^* cm
46412	340.986	536.480	0.168011	576	2.1

For Data 1, the results are summarized in Tables 11 where for each of the mentioned DART buoy's locations the forecast of travel time t_k^* (in minutes) of the wave of maximum height and its height H_k^* (in centimetres) are shown; the subscript k shows that the forecast is based on measurements obtained from k buoys.

The actual travel time t_* and height H_* are repeated from Table 1.

Table 11. For Data 1: the forecasts based on the model (4.1.1).

Buoy	t_1^*	t_2^*	t_3^*	t_*	H_1^*	H_2^*	H_3^*	H_*
32411	192	-	-	198	3.9	-	-	1.7
51406	396	411	-	444	2.8	2.3	-	3.9
46412	518	540	576	624	2.4	2.0	2.1	2.0

6.2. The forecast based on Data 2

The method of Subsection 6.1 is applied to the waves recorded at a number of DART buoys. The data obtained from the records are shown in Table 2. The results of forecasting are presented in Table 12 and figure 3.

Table 12. For Data 2: the forecasts based on the model (4.1.1).

Buoy	t_2^*	t_3^*	t_4^*	t_*	H_2^*	H_3^*	H_4^*	H_*
46413	151	-	-	154	4,4	-	-	5,7
46408	183	184	-	200	4,0	4,4	-	4,5
46419	366	374	391	438	2,9	3,1	3,1	1,6

6.3. The forecast based on Data 3

The Data 3 obtained from the records are shown in Table 3. The results of forecasting are presented in Table 13.

Table 13. For Data 3: the forecasts based on the model (4.1.1).

Dart	t_1^*	t_2^*	t_3^*	t_*	H_1^*	H_2^*	H_3^*	H_*
46408	187	-	-	238	7.8	-	-	7.5
46402	211	257	-	270	7.3	6.6	-	10.0
46403	243	295	307	365	6.9	6.2	6.8	7.5

The forecast results show earlier arrivals of the WMH ($t^* < t_*$). For Data 1 the percentage errors equal $(1 - 192/198) \cdot 100\% = 3.0\%$ for buoy 32411, $(1 - 411/444) \cdot 100\% = 7.4\%$ for buoy 51406, and $(1 - 576/624) \cdot 100\% = 7.8\%$ for buoy 46412.

The estimates H_i^* of the maximum wave heights at the buoys exhibit no regularity: at the buoys, some of the estimates are close to the actual values H_* , and some of the estimates deviate from H_* . The range of the deviations $|H_i^* - H_*|$ is from 0 to H_* . Maximum water elevation in the wave origin is $h = 0.13$ m for Data 1, $h = 0.14$ m for Data 2, and $h = 0.33$ m for Data 3. The value of the ratio $h/|a|$ is of order $10^{-6} - 10^{-5}$. We are not aware of instrumental measurements of water elevation in a wave origin.

Duration t of the wave origin formation is estimated as $t = 51$ s for Data 1, $t = 58$ s for Data 2, and $t = 47$ s for Data 3.

We are not aware of any theoretical estimates of the duration of wave origin formation, but in the available literature analogous estimates are given for the earthquakes: typical earthquake with elastic energy release lasts 10 s (Watts 2001), "The duration of the rupture process is about 100 s, unusually long for its size" (Satake 1995) (i.e., the size of the 1992 Nicaragua earthquake source). Mean duration of an earthquake rupture is about 23 s (Burimskaya, Levin & Soloviev 1981).

In passing. By the linear theory, speed c of harmonic waves, their wavelength l , and water depth d are related as follows

$$c^2 = \frac{gl}{2\pi} \tanh \frac{2\pi d}{l}.$$

For Data 1 the length of the wave of maximum height is 91 km, its speed $V \approx 750$ km/h = 208 m/s.

At this values we get

$$\tanh \frac{2\pi d}{l} = 0,305640, \quad \frac{2\pi d}{l} = 0,32, \quad d = 4,8 \text{ km}.$$

REFERENCES

1. Mindlin, I.M.: Integrodifferential Equations in Dynamics of Heavy Layered Liquid, Nauka*Fizmatlit, Moscow, 304 p, (1996) (Russian).
2. Mindlin, I.M.: Deep-water gravity waves: nonlinear theory of wave groups. arXiv:1406.1681v1 [physics.ao-ph], 30 p, (6 Jun 2014)
3. Satake, K. Linear and nonlinear computations of the 1992 Nicaragua earthquake tsunami. Pure and Appl. Geophys. vol. 144, 3/4, 455-470, (1995).
4. Watts, Ph. Some opportunities of the landslide tsunami hypothesis. Science of tsunami hazards, vol.19, 3, 126-149, (2001).
5. Burimskaya, R.N., Levin, B.V. & Soloviev, S.L. A kinematic criterion for tsunamigenity of an underwater earthquake. Dokl. Akad. Nauk. SSSR. **261**, 6, 1325-1330, (1981) (Russian).